DOI 10.1007/s10946-019-09822-3
Journal of Russian Laser Research, Volume 40, Number 5, September, 2019

TWISTED KINETIC PLASMA WAVES

D. R. Blackman,[1] R. Nuter,[1] Ph. Korneev,[2,3] and V. T. Tikhonchuk[1,4*]

[1] *CELIA, University of Bordeaux, CNRS, CEA*
Talence 33405, France

[2] *National Research Nuclear University MEPhI*
Kashirskoe Shosse 31, Moscow 115409, Russia

[3] *Lebedev Physical Institute, Russian Academy of Sciences*
Leninskii Prospect 53, Moscow 119991, Russia

[4] *ELI-Beamlines, Institute of Physics, Czech Academy of Sciences*
Dolní Břežany 25241, Czech Republic

*Corresponding author e-mail: tikhonchuk @ u-bordeaux.fr

Abstract

Similarly to electromagnetic waves, plasma waves can also carry an orbital angular momentum. A key distinction from electromagnetic waves is that plasma waves are intrinsically coupled to electrons and may deposit their momentum with electrons, resulting in their secular motion and generation of quasistatic magnetic fields. In this paper, we present an analysis of kinetic plasma waves carrying an orbital angular momentum in the paraxial approximation by considering the energy and momentum exchange between the wave and electrons and the average electron motion induced by plasma wave damping.

Keywords: plasma waves, Landau damping, orbital angular momentum, paraxial approximation.

1. Introduction

The kinetic theory of plasma waves and their interaction with charged particles were the favorite research subjects of Viktor Pavlovich Silin. He dedicated many seminal papers to the properties of plasma waves, plasma wave turbulence, and their applications for plasma heating and particle acceleration under various conditions. In this paper, we consider a relatively new type of plasma waves that carry an orbital angular momentum. These are collective electron oscillations propagating along a symmetry axis z and spatially limited in the radial direction. A particularity of these waves consists in their capacity to carry, in addition to the axial momentum, an orbital angular momentum, that is, the plasma wave electric field having an azimuthal component, which is a periodic function of the azimuthal angle θ in the cylindrical coordinate system.

Electromagnetic waves carrying an orbital angular momentum (OAM) were introduced by Allen et al. [1] and rapidly found various applications in optics for compact information storage and nanoscale imaging and manipulation [2]. Such waves have a form of radially limited beams described by Laguerre–Gaussian functions, which are eigenmodes of the paraxial optics equation in the cylindrical coordinates. Recent publications show that the interference of two such electromagnetic beams in plasma may excite plasma oscillations, transfer to electrons a part of their orbital momentum, and create quasistatic magnetic fields [3–6].

Manuscript submitted by the authors in English on July 15, 2019.

1071-2836/19/4005-0419©2019 Springer Science+Business Media, LLC

Plasma waves carrying an orbital momentum have also been described within the Laguerre–Gaussian framework in the hydrodynamic approximation [7]. However, the hydrodynamic model cannot describe such processes as the Landau damping, particle acceleration, and magnetic field generation. A kinetic description is required, but it is more complicated as transverse motion of electrons results in mode coupling. A kinetic theory of plasma waves in the cylindrical geometry has been developed by Mendonça [8], who however neglected coupling of angular modes. Recently we developed a consistent theory of kinetic OAM plasma waves [6]. We accounted for mode coupling in the paraxial approximation by considering the ratio of the plasma wavelength $\lambda = 2\pi/k$ to the wave radial width w_b as a small parameter, $1/kw_b \ll 1$. We showed that the presence of an orbital angular momentum and corresponding radial structure of the plasma wave change its dispersion and damping.

In this paper, we briefly recall the formal theory of OAM plasma waves and present a physical interpretation of the resonant wave–particle interaction, which results in the transfer of energy and momentum between the wave and the particles. In particular, the resonantly-accelerated electrons carry an angular momentum, and the corresponding azimuthal electric current produces a quasistatic axial magnetic field. The analytical expressions are illustrated and confirmed with intense three-dimensional numerical simulations.

2. Dispersion Equation for the Plasma Wave in a Cylindrical Geometry

An electric field $\mathbf{E}$ of the electromagnetic wave propagating in plasma along the z-axis can be represented in the paraxial approximation as follows:

$$\mathbf{E} = \mathbf{e}\ \mathrm{Re}\{E_0(\tau)\ \exp(-i\omega t + ikz)\, U(z, r, \theta)\},$$

where $\mathbf{e}$ is the constant polarization unitary vector, ω is the wave frequency, $k = \omega/c$ is the axial wave number, $\tau = t - z/v_g$ is the copropagating time, $E_0(\tau)$ is the amplitude slowly changing in time, v_g is the group velocity, and the scalar function U describes the waveform in the transverse plane. The latter is a solution of the paraxial wave equation

$$(2ik\partial_z + \nabla_\perp^2)\, U = 0,$$

where we neglect the second derivative in z assuming the paraxial condition $kw_b \gg 1$. In the cylindrical geometry, the function U can be developed in a series of eigenmodes, which are the Laguerre–Gaussian (LG) functions [1],

$$U(z, r, \theta) = \sum_{p,l} c_{p,l} F_{p,l}(X)\ \exp\left(il\theta + i\varphi_{p,l} + iXz/2z_R\right). \tag{1}$$

Here, $X = r^2/w_b^2$ is the normalized radial coordinate, $w_b(z) = w_{b,0}\sqrt{1 + z^2/z_R^2}$ is the beam width, $w_{b,0}$ is the beam waist at the focal point, $z_R = kw_{b,0}^2$ is the Rayleigh length, $\varphi_{p,l}(z) = -(2p + |l| + 1)\arctan(z/z_R)$ is the Gouy phase, $f(z) = z + z_R^2/z$ is the wavefront curvature, and $c_{p,l}$ are coefficients slowly depending on time. The radial wave number $p \geq 0$ is an integer that numerates radial modes. The integer l could be positive or negative, and it numerates the orbital angular momentum (OAM).

The radial eigenfunction $F_{p,l}$ is the Laguerre–Gauss (LG) mode,

$$F_{p,l}(X) = \sqrt{\frac{p!}{(|l|+p)!}} X^{|l|/2} L_p^{|l|}(X)\, \mathrm{e}^{-X/2},$$

where $L_p^{|l|}(X)$ is a generalized, or associated, Laguerre polynomial of degrees p and l. The set of functions $F_{p,l}$ are orthogonal and normalized according to the following relation:

$$\int_0^\infty dX\, F_{p,l}(X)\, F_{p',l}(X) = \delta_{p,p'},$$

where $\delta_{p,p'}$ is the Kronecker symbol.

A small amplitude plasma wave in a constant density plasma can be also described in the LG formalism. The electrostatic potential Φ and the electron distribution function f_e satisfy the Poisson and Vlasov equations, respectively. For a monochromatic plasma wave, with frequency ω and wave number k, in the paraxial approximation, $1/kw_{b,0} \ll 1$, the solution is expanded in a series of LG functions as follow:

$$\Phi = \mathrm{Re} \sum_{p,l} \phi_{p,l} F_{p,l}(X) \exp\left(-i\omega t + ikz + il\theta + i\varphi_{p,l} + iXz/2z_R\right), \tag{2}$$

$$\delta f_e = \mathrm{Re} \sum_{p,l,m} f_{p,l}^{(m)}(v_z, v_\perp) F_{p,l}(X) \exp\left(-i\omega t + ikz + il\theta - im\theta_v + i\varphi_{p,l} + iXz/2z_R\right), \tag{3}$$

where δf_e is deviation of the electron distribution function from a Maxwellian distribution function f_{e0} with density $n_{e,0}$ and temperature T_e, and θ_v is the angle of the electron velocity with the reference direction in the transverse plane. The Poisson equation is linear; thus, it provides relations between the coefficients of the same mode,

$$\phi_{p,l} = -\frac{e}{\varepsilon_0 k^2} \int d\mathbf{v}\, f_{p,l}(\mathbf{v}).$$

The situation is more complicated with the Vlasov equation, which cannot be separated in a set of independent equations because the gradient operators $v_z\partial_z$ and $\mathbf{v}_\perp \cdot \nabla_\perp$ couple the modes with different orbital momenta and radial structure. The use of a small parameter $1/kw_b \ll 1$ allowed us [6] to account for coupling of the mode p, l to close neighbors with orbital momentum $l \pm 1$ and radial number $p \pm 1$. Excluding then the first-order terms, the following expression for the electron distribution function averaged over the azimuthal angle has been obtained:

$$f_{p,l}^{(0)} = \left[-1 + \frac{\omega\,(\omega - kv_z)}{(\omega - kv_z)^2 + Q_{p,p}^{(l)} v_\perp^2 / w_b^2}\right] e\phi_{p,l} \partial_\varepsilon f_{e0}. \tag{4}$$

The denominator in the second term in the square brackets of this equation accounts for the shift of the resonance condition $\omega = kv_z$ due to the transverse structure of the plasma wave with the coefficient

$$Q_{p,p}^{(l)} = -\left(1 + \frac{z^2}{z_R^2}\right)\left(p + \frac{|l|+1}{2}\right).$$

By substituting expression (4) for the electron distribution function in the Poisson equation, the dispersion equation for the twisted plasma wave can be obtained. In the case $|z| < z_R$ considered in what follows, it reads

$$\varepsilon(\omega, k) = 1 + \frac{e^2}{\varepsilon_0 k^2} \int d\mathbf{v} \left[-1 + \frac{\omega\,(\omega - kv_z)}{(\omega - kv_z)^2 - (2p + |l| + 1)v_\perp^2/2w_{b,0}^2} \right] \partial_\varepsilon f_{e0} = 0. \tag{5}$$

The solution to this equation in the limit $\omega \gg kv_{th}$, where $v_{th} = \sqrt{T_e/m_e}$ is the electron thermal velocity, can be found using a standard expansion procedure. The real part of the dispersion equation (5) gives the following expression for the plasma wave dispersion:

$$\omega \approx \omega_{pe} \left(1 + \frac{3}{2} k^2 \lambda_{De}^2 + \frac{2p + |l| + 1}{2k^2 w_{b,0}^2} \right), \tag{6}$$

where $\omega_{pe} = \sqrt{e^2 n_{e0}/m_e \varepsilon_0}$ is the plasma frequency and $\lambda_{De} = v_{th}/\omega_{pe}$ is the electron Debye length. The last term in the parenthesis accounts for the OAM and final radial extension of the plasma wave. It makes a positive nonthermal contribution to the wave dispersion.

Taking the residue in the resonance terms on the right-hand side of Eq. (5), one finds an expression for the plasma wave damping. The Landau resonance in the case of plane wave $v_z = \omega/k$ splits into two resonances $v_z^{\pm} = (\omega/k) \pm (v_\perp/kw_{b,0})\sqrt{p + (|l| + 1)/2}$ shifted with respect to the axial phase velocity. Calculation of corresponding integrals leads to the following expression for the plasma wave damping rate $\gamma = -\operatorname{Im}\omega$:

$$\frac{\gamma}{\omega} \approx \sqrt{\frac{\pi}{8}} \frac{1}{k^3 \lambda_{De}^3} \exp\left(-\frac{\omega^2}{2k^2 v_{th}^2} \right) R\left(\frac{\sqrt{p + (|l| + 1)/2}}{k^2 \lambda_{De} w_{b,0}} \right). \tag{7}$$

Here, the function $R(\xi) = 1 + \sqrt{\pi/2}\,\xi \exp(-\xi^2/2) \operatorname{Erf}(\xi/\sqrt{2})$ accounts for the OAM with Erf being the error function. Graphical representations of these two functions with comparisons to the standard dispersion relation and damping are presented in Fig. 1. The OAM carried by plasma waves results in a notable increase in the dispersion. The contribution of OAM to the wave damping is visible for a beam width $w_{b,0}$ smaller than $20\,\lambda_{De}$.

3. Structure of a Vortical Plasma Wave

As an example of twisted plasma wave considered in the previous section, here we consider the structure of a single mode p, l within the Rayleigh zone $|z| < z_R$. The electric potential (2) contains only one term characterized by the amplitude $\phi_{p,l}$:

$$\Phi(z, r, \theta, t) = \phi_{p,l} F_{p,l}(X) \cos(kz - \omega t + l\theta). \tag{8}$$

The electric field can be found taking the gradient of the potential. The axial field $E_z = k\phi_{p,l} F_{p,l} \sin(kz - \omega t + l\theta)$ dominates, and the transverse fields $E_r = -(2r/w_{b,0}^2)\phi_{p,l} F'_{p,l} \cos(kz - \omega t + l\theta)$ and $E_\theta = (l/kr)E_z$ are smaller by a factor $1/kw_{b,0} \ll 1$. The radial field has a phase shifted by a quarter of a period with respect to the azimuthal and axial fields.

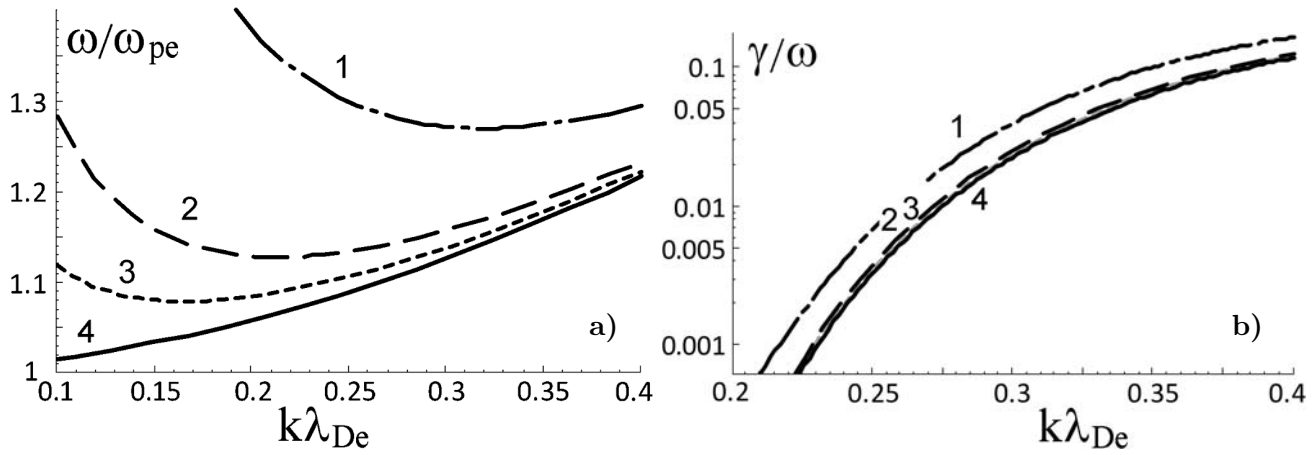

Fig. 1. Dispersion (a) and damping (b) of the plasma wave with $p = 0$ and $l = 1$ calculated using Eqs. (6) and (7). The wave width $w_{b,0}/\lambda_{De} = 8$ (curve 1, dash-dotted), 18 (curve 2, dashed), 30 (curve 3, dotted), and 1,000 (curve 4, solid).

The electron distribution function in the first order over the paraxial parameter can be presented in the following explicit form:

$$\delta f_e = -e\phi_{p,l}\partial_\varepsilon f_{e0} F_{p,l}\cos(kz - \omega t + l\theta) + \frac{\omega e\phi_{p,l}\partial_\varepsilon f_{e0}}{(\omega - kv_z)^2 - (2p + |l| + 1)v_\perp^2/2w_{b,0}^2}$$
$$\times\left[\left(\omega - kv_z + \frac{v_\theta l}{r}\right)F_{p,l}\cos(kz - \omega t + l\theta) - 2\frac{v_r r}{w_{b,0}^2}F'_{p,l}\sin(kz - \omega t + l\theta)\right], \qquad (9)$$

where F' is the derivative of the LG function with respect to its argument X. Coupling of the dominant part of the distribution function $f_{p,l}^{(0)}$ to neighboring modes $f_{p,l\pm1}^{(\pm1)}$ and $f_{p\mp1,l\pm1}^{(\pm1)}$ results in the appearance of azimuthal v_θ and radial v_r electron velocities in terms of the first order on the paraxial parameter [6]. This expression can be used for calculation of the moments of the electron distribution function. The lowest moments, the perturbation of density and electric current, can also be found directly from the Poisson and Ampere equations. For further analysis, we are interested in the electron density perturbation $e\delta n_e = -k^2\varepsilon_0\Phi$, the axial velocity $u_z = -ek\Phi/m_e\omega$, and the azimuthal velocity $u_\theta = -el\Phi/m_e r\omega$.

These expressions take a simpler explicit form for the lowest mode $p = 0$ and $l = 1$, where the corresponding radial function reads $F_{0,1} = X^{1/2}\mathrm{e}^{-X/2}$. The electric potential (8) is characterized by a dimensionless amplitude $a_0 = e\phi_{0,1}/m_e c^2$,

$$e\Phi/m_e c^2 = a_0(r/w_{b,0})\,\mathrm{e}^{-r^2/2w_{b,0}^2}\,\cos(kz - \omega t + \theta).$$

The perturbation of the electron distribution function given by Eq. (4) reads

$$\frac{\delta f_e}{f_{e0}} = a_0\frac{m_e c^2}{T_e}\,\frac{r}{w_{b,0}}\,\mathrm{e}^{-r^2/2w_{b,0}^2}\cos(kz - \omega t + \theta) - a_0\frac{m_e c^2}{T_e}\,\frac{\omega}{(\omega - kv_z)^2 - v_\perp^2/w_{b,0}^2}\,\mathrm{e}^{-r^2/2w_{b,0}^2}$$
$$\times\left[\left(\omega - kv_z + \frac{v_\theta}{r}\right)\frac{r}{w_{b,0}}\cos(kz - \omega t + \theta) + \frac{v_r}{w_{b,0}}\left(\frac{r^2}{w_{b,0}^2} - 1\right)\sin(kz - \omega t + \theta)\right].$$

The analytical results presented here were confirmed by numerical calculations using the particle-in-cell (PIC) code OCEAN [9]. A three-dimensional box containing 480×480×160 cubic cells with sides of length $\pi/20k$ is filled with a uniform plasma with fixed ions and electrons having temperature $T_e = 0.03\, m_e c^2$; 100 particles per cell are used to achieve a signal-to-noise ratio sufficient for measuring damping. The boundary condition along the propagation axis is absorbing, while in the transverse directions they are reflecting for both fields and particles. In order to facilitate a simple periodic plasma wave with OAM, the Gouy phase and front curvature are ignored for this analysis assuming $|z| < z_R$.

Simulations are run with a mode $p = 0$, $l = 1$ having a wave number $k = 1.9\,\omega_{pe}/c$ corresponding to the parameter $k\lambda_{De} = 0.33$ and a frequency ω close to the plasma frequency. The length of the box, L_z, was chosen so that it fits exactly four wavelengths with $kL_z = 8\pi$. The width of the plasma wave $w_{b,0} = 6/k$ is chosen so that the additional dispersion owing to OAM in Eq. (5) is small, $\omega/\omega_{pe} = 1.17$, with 3% coming from the last term, while the OAM contribution to the damping (7) increases it by a factor of 1.28. The expected damping is $\gamma/\omega = 0.038$; see curve 2 in Fig. 1.

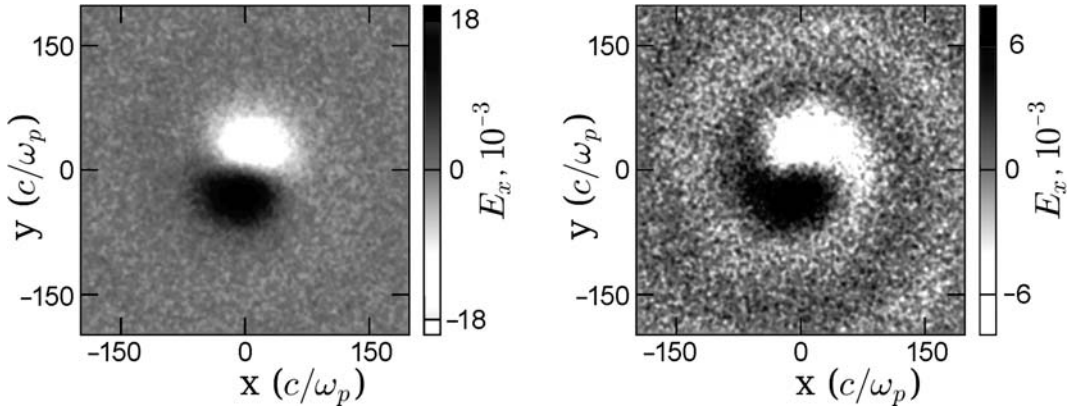

Fig. 2. Results from OCEAN PIC simulation. Plots show transverse slices taken halfway along the simulation box of E_x normalized to the plasma field $E_p = m_e c\omega_{pe}/e$. The left-hand side plot shows the simulation at the time the amplification process stops at $t \simeq 30/\omega_{pe}$ and so is at a maximum amplitude; the right-hand side plot shows the simulation at time $\sim 70/\omega_{pe}$ during the damping process.

An electric field calculated from the potential described by Eq. (8) is imposed volumetrically on each time step, with the dimensionless amplitude a_0 increasing linearly in time from zero to the maximum value $a_0 = |E_x|/E_p \simeq 0.02$ over five plasma periods, $2\pi/\omega_{pe}$. After that time, the wave evolved freely in plasma without any driver over more than 20 periods, with the amplitude decaying exponentially.

Figure 2 shows two transverse slices of the axial electric field from halfway along the simulation box, the first plot showing E_x immediately after amplification at the maximum amplitude, and the second plot ~ 10 plasma periods later. The first plot shows a clean LG mode while the second plot shows a spiral shaped perturbation, which is visible while the wave is damping. It is likely this is due to electrons carrying the orbital angular momentum away from the plasma wave as it decays.

Values for the plasma wave frequency and Landau damping are found from the wave form calculated with the PIC code. Figure 3 a shows the spectrum of excited plasma wave calculated over a time of about 10 periods in the interval delimited in panel 2 with two vertical dashed lines. The measured wave frequency is in good agreement with the values expected from the dispersion relation (6). The procedure for damping rate calculation is explained in Fig. 3 b: the points are taken at the peaks of the current and electric field and fitted to an exponential function. These points are taken at $kr = 1.9\,\pi$ to capture

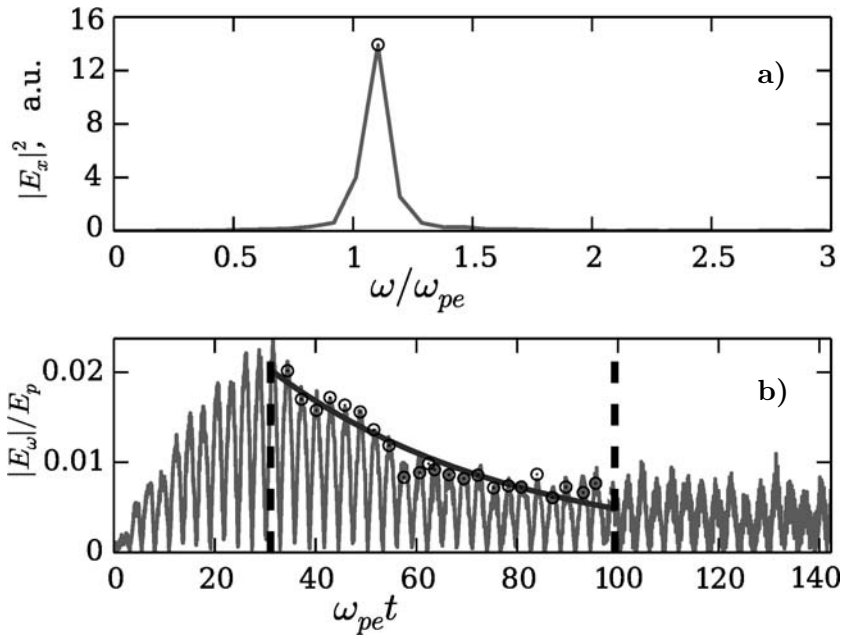

Fig. 3. Spectrum (a) and waveform (b) of the plasma waves obtained from the PIC calculation. Panel a shows the wave spectrum measured in the time interval shown with vertical dashed lines in panel b. The frequency value $\omega/\omega_{pe} = 1.17 \pm 0.05$, where the error comes from the spectral resolution. Panel b shows the absolute value of electric field as a function of time sampled at a position $kx = 4.25\,\pi$ and $kr = 1.9\,\pi$, where the maximum amplitude is expected but with fixed $\theta = \pi/2$ to capture oscillatory behavior. The time interval between $t = 0$ and $t \simeq 30/\omega_{pe}$ (up to the fist black dashed line from the left) is the amplification time. The interval between the two black dashed lines is used for fitting the wave amplitude to the exponential law, $a(t) = a_0 \mathrm{e}^{-\gamma t}$ (shown as small crosses).

the maximum amplitude and at $kx/\pi = 3.25$, 3.75, 4.25, 4.75 and $\theta/\pi = 0$, 1/2, 1, 3/2. The decay in amplitude of both longitudinal current and electric field is measured independently and produced similar results. The value calculated from all points gives $\gamma/\omega = 0.036 \pm 0.003$, which is in fair agreement with the expected value of 0.038. However, taking the lowest half of the data gives a smaller value of $\gamma/\omega = 0.027 \pm 0.002$. The nonuniformity of damping across the simulation box is likely due to the relatively high noise level and nonuniform temperatures at the absorbing boundaries. At later time $\omega_{pe}t > 100$, the wave evolution enters into the nonlinear phase, and the wave amplitude is stabilized due to the energy exchange with trapped particles.

4. Interaction of a Twisted Plasma Wave with Resonant Particles

The twisted plasma wave carries the orbital angular momentum in addition to the energy and momentum of the ordinary plasma wave. The time-averaged energy density $W = \varepsilon_0 k^2 \phi_{p,l}^2 F_{p,l}^2/2$ is equally distributed between the field and the particles. However, only particles contribute to the time-averaged momentum of the plasma mode $\mathbf{P} = \langle \delta n_e m_e \mathbf{u} \rangle$. Consequently, the expression for the axial momentum reads $P_z = \varepsilon_0 k^3 \phi_{p,l}^2 F_{p,l}^2/2\omega$. Similarly we obtain an expression for the axial component of the orbital momentum,

$$L_z = \langle r P_\theta \rangle = \varepsilon_0 k^2 l \phi_{p,l}^2 F_{p,l}^2/2\omega. \tag{10}$$

Performing integration in the transverse plane, we find the total energy per unit length carried by the plasma wave $\mathcal{W} = \pi\varepsilon_0 k^2 w_b^2 \phi_{p,l}^2/2$, the orbital momentum per unit length $\mathcal{P}_z = \pi\varepsilon_0 k^3 w_b^2 \phi_{p,l}^2/2\omega$, and the total orbital momentum $\mathcal{L}_z = \pi k^2 l w_b^2 \varepsilon_0 \phi_{p,l}^2/2\omega$. The last two quantities depend on the sign of the axial wave number k and the orbital momentum l, respectively.

The interaction of a plasma wave with resonant particles results in its absorption. This process corresponds to an irreversible transfer of the wave energy and momentum to electrons. The rate of energy gain by electrons can be evaluated by calculating the period-averaged work performed by the electric field on the current: $dW/dt = \langle \mathbf{E} \cdot \mathbf{j} \rangle$. Evaluating the current from expression (9) for the electron distribution function, one can demonstrate that $\langle \mathbf{E} \cdot \mathbf{j} \rangle = 2\gamma W$, that is, the wave damping (7) defines the rate of energy transfer. Similarly, by calculating the average longitudinal force $\langle -e\delta n_e E_z \rangle$ and the longitudinal component of the torque $\langle -er\delta n_e E_\theta \rangle$ one can demonstrate that the axial momentum and orbital momentum are transferred to electrons with the same rate: $d\mathcal{P}_z/dt = 2\gamma \mathcal{P}_z$ and $d\mathcal{L}_z/dt = 2\gamma \mathcal{L}_z$.

However, the general expression for the wave damping (7) does not show how the absorbed energy and momentum are distributed between the particles. In order to demonstrate the dissipation process explicitly, we employ a microscopic approach following the method presented in [10, 11].

Let us calculate the gain of the orbital momentum of an electron, $l_z = m_e r v_\theta$, in the plasma wave field in the first order over a short interval of time Δt. The increment of the orbital angular momentum contains two terms, $\Delta l_z = m_e \Delta r v_\theta + m_e r \Delta v_\theta$, but only the second one needs to be calculated. The first term is imparted to the electron azimuthal velocity and will disappear after integration over all velocities with the electron distribution function. The increment of the azimuthal velocity can be calculated from the electron equation of motion

$$d_t v_\theta = -(v_r v_\theta/r) - eE_\theta/m_e,$$

where $E_\theta = -r^{-1}\partial_\theta \Phi$. The first term on the right-hand side is imparted to the radial and azimuthal velocities and will disappear after integration. For integration of the second term, one has to account for the variation of coordinates along the electron trajectory. In the lowest order, we have

$$z(t) = z_0 + v_z t, \qquad \theta(t) = \theta_0 + v_\theta t/r, \qquad r(t) = r_0 + v_r t.$$

By integrating then the azimuthal electric field over the time interval Δt, we find the increment of the azimuthal velocity and the orbital momentum; the latter is

$$\Delta l_z = el\phi_{p,l} \frac{F_{p,l}}{kv_z + v_\theta l/r - \omega} \big\{ \cos[kz_0 + l\theta_0 + \big(kv_z + (v_\theta l/r) - \omega\big)\Delta t] - \cos(kz_0 + l\theta_0) \big\}.$$

In order to account for the contribution of all electrons, we integrate this expression over the electron distribution function f_{e0}. The total gain of the angular momentum comprises two terms: (i) increase in the orbital momentum of the electrons having the initial velocity $\mathbf{v}$ and gaining the velocity increment $\Delta\mathbf{v}$, and also (ii) reciprocal decrease of the orbital momentum of the electrons having the initial velocity $\mathbf{v} + \Delta\mathbf{v}$ and decreasing by $\Delta\mathbf{v}$,

$$\Delta L_z = \int d\mathbf{v}\, \Delta l_z [f_{e0}(\mathbf{v}) - f_{e0}(\mathbf{v} + \Delta\mathbf{v})] \approx -m_e \int d\mathbf{v}\, \Delta l_z \Delta\mathbf{v} \cdot \mathbf{v}\, \partial_\varepsilon f_{e0}(\varepsilon). \tag{11}$$

Before taking the integral over velocities in this expression, we need to average the product $\Delta l_z \Delta\mathbf{v}$ over the initial position of the electron, z_0 and θ_0, over one wave period. The axial and azimuthal components of the electron velocity increment oscillate in phase: $\Delta v_z = (kr/l)\Delta v_\theta$. Conversely, the radial part of the

electron velocity increment is shifted by a quarter of period with respect to the azimuthal component. It does not contribute to the averaged expression for the increment of the electron orbital momentum,

$$\Delta L_z = -2kle^2\phi_{p,l}^2 F_{p,l}^2 \int d\mathbf{v}\, \frac{(v_z + v_\theta l/kr)\partial_\varepsilon f_{e0}}{[kv_z + (v_\theta l/r) - \omega]^2} \sin^2[\big(kv_z + (v_\theta l/r) - \omega\big)\Delta t/2]. \tag{12}$$

This expression can be further simplified by taking the limit $\Delta t \to 0$ and using the following relation:

$$\lim_{\Delta t\to 0} \int_{-\infty}^{\infty} da\, \frac{\sin^2(a\Delta t)}{a^2} = \Delta t \int_{-\infty}^{\infty} d\xi\, \frac{\sin^2\xi}{\xi^2} = \pi\Delta t.$$

Correspondingly, the rate of the orbital angular momentum gain by electrons from the wave reads

$$\frac{dL_z}{dt} = -\pi l\omega e^2\phi_{p,l}^2 F_{p,l}^2 \int d\mathbf{v}\, \delta\big(kv_z + (v_\theta l/r) - \omega\big)\, \partial_\varepsilon f_{e0}\,. \tag{13}$$

The delta-function selects the integral in the velocity space along the resonance line $kv_z + (v_\theta l/r) - \omega = 0$. For a given absolute value of the transverse velocity $v_\perp$, there are two values of the azimuthal angle, where this condition can be satisfied. By performing integration over the velocity azimuthal angle θ_v and using expression (10) for the orbital momentum, we find

$$\frac{1}{L_z}\frac{dL_z}{dt} = -\frac{e^2\omega^2}{\varepsilon_0 k^2} \int d\mathbf{v}\, \frac{\partial_\varepsilon f_{e0}}{\sqrt{(v_\perp l/r)^2 - (kv_z - \omega)^2}}. \tag{14}$$

As one can see, in the square root term under the integral, only a narrow range of electron velocities $\Delta v_z/v_{th} \sim l/kr \ll 1$ contributes to this expression.

For a Maxwellian distribution function f_{e0}, the remaining integrals can be also calculated. That gives us the following expression for the rate of the orbital momentum gain by electrons:

$$\frac{1}{L_z}\frac{dL_z}{dt} \approx \sqrt{\frac{\pi}{2}}\frac{\omega}{k^3\lambda_{De}^3} \exp\left(-\frac{\omega^2}{2k^2v_{th}^2} + \frac{l^2}{2k^2\lambda_{De}r}\right). \tag{15}$$

Owing to the orbital momentum conservation, the OAM gained by electrons is equal to the OAM lost by the wave. Therefore, expression (15) with the opposite sign defines the rate of the plasma wave orbital angular momentum damping rate, i.e., $\dfrac{dL_z}{dt}\dfrac{1}{L_z} = 2\gamma$. In the limit $k^2\lambda_{de}r \gg l^2$, this corresponds to a standard expression for the Landau damping rate. In the opposite limit, $k^2\lambda_{de}r \lesssim l^2$, the damping rate is larger, and there is a difference between Eq. (7) and (15). This difference is partially explained by the fact that in deriving the latter expression we did not perform averaging over the radial structure of the wave.

Similar expressions can be obtained for the rate of energy and axial-momentum losses of the plasma wave. This means that the axial momentum, orbital angular momentum, and energy are dissipated with the same rate, and the resonance wave–particle interaction transfers them irreversibly from the bulk-motion adiabatic particles to the resonant particle moving with the phase velocity of the wave.

5. Conclusions

The analysis presented in this paper shows that, similarly to electromagnetic waves, the electrostatic wave may also carry an orbital angular momentum and effectively transfer it to resonant particles. The

method developed for Langmuir plasma waves can be readily extended to ion acoustic and electrostatic waves propagating along an external magnetic field. These waves can be excited by beating two co- or counter-propagating electromagnetic waves carrying OAM and thus facilitate coupling of the wave momentum to plasma particles.

Imparting of axial and orbital angular momenta to electrons corresponds to excitation of the axial and azimuthal quasistatic electric currents. Modulation of the plasma wave currents by the density perturbations, as demonstrated in [6], results in excitation of a quasistatic magnetic field. It is of a second order on the wave amplitude and has azimuthal B_θ and axial B_z components with magnetic field lines forming helices. For a sufficiently high-amplitude plasma wave, these magnetic fields can be used for collimation and guiding energetic electrons, for example, in the wake field acceleration scheme. The magnetic fields are related to the mechanical momenta according to the Ampere law: $B_\theta \simeq -(\mu_0 e/m_e)\,\mathcal{P}_z/2\pi r$ and $\Psi_z = 2\pi \int B_z r\,dr \simeq -(\mu_0 e/2m_e)\mathcal{L}_z$, where μ_0 is the vacuum magnetic permeability.

The excitation of a twisted plasma wave with orbital angular momentum $l = 2$ was described in [5]. Two copropagating electromagnetic waves with opposite OAM ± 1 were used to resonantly excite a Langmuir wave in a plasma with density $2.5 \cdot 10^{-3}$ of the critical density. The chosen parameters, however, correspond to a small value of parameter $kw_b = 0.2$, which is opposite to the paraxial condition $kw_b \gg 1$. Consequently, the plasma wave was strongly damped, and the authors observed a relatively weak axial magnetic field with induction of a few teslas. Excitation of a plasma wave in the paraxial regime offers higher wave amplitudes and stronger magnetic fields.

Acknowledgments

This work was granted access to HPC resources of TGCC under the allocation A0010506129 made by GENCI. We acknowledge PRACE for awarding us access to resource Joliot Curie-SKL based in France at TGCC Center. The authors acknowledge support from MEPhI Academic Excellence Project (Contract No. 02.a03.21.0005-27.08.2013) and from the Project ELITAS (ELI Tools for Advanced Simulation) CZ.02.1.01/0.0/0.0/16_013/0001793 from the European Regional Development Fund.

References

1. L. Allen, M. W. Beijersbergen, R. J. C. Spreeuw, and J. P. Woerdman, *Phys. Rev. A*, **45**, 8185 (1992).
2. Q. Zhan, *Adv. Opt. Photon.*, **1**, 1 (2009).
3. J. Vieira and J. T. Mendonça, *Phys. Rev. Lett.*, **112**, 215001 (2014).
4. J. Vieira, R. M. G. M. Trines, E. P. Alves, et al., *Nature Commun.*, **7**, 10371 (2016).
5. Y. Shi, J. Vieira, R. M. G. M. Trines, et al., *Phys. Rev. Lett.*, **121**, 145002 (2018).
6. D. R. Blackman, R. Nuter, Ph. Korneev, and V. T. Tikhonchuk, *Phys. Rev. E*, **100**, 013204 (2019).
7. J. T. Mendonça, S. Ali, and B. Thidé, *Phys. Plasmas*, **16**, 112103 (2009).
8. J. T. Mendonça, *Phys. Plasmas*, **19**, 112113 (2012).
9. R. Nuter and V. Tikhonchuk, *Phys. Rev. A*, **87**, 043109 (2013).
10. F. F. Chen, *Introduction to Plasma Physics and Controlled Fusion*, Plenum Press, New York (1984), Vol. 1, p. 256.
11. J.-M. Rax, *Physique des Plasmas*, Dunod, Paris (2005), p. 297.